# Localized Spins on Graphene

P. S. Cornaglia, Gonzalo Usaj, and C. A. Balseiro

*Centro Atómico Bariloche and Instituto Balseiro, CNEA, 8400 Bariloche, Argentina*
*and Consejo Nacional de Investigaciones Científicas y Técnicas (CONICET), Argentina*

(Received 10 September 2008; published 27 January 2009)

The problem of a magnetic impurity, atomic or molecular, absorbed on top of a carbon atom in otherwise clean graphene is studied using the numerical renormalization group. The spectral, thermodynamic, and scattering properties of the impurity are described in detail. In the presence of a small magnetic field, the low-energy electronic features of graphene make it possible to inject spin-polarized currents through the impurity using a scanning tunneling microscope. Furthermore, the impurity scattering becomes strongly spin dependent and for a finite impurity concentration it leads to spin-polarized bulk currents and a large magnetoresistance. In gated graphene the impurity spin is Kondo screened at low temperatures. However, at temperatures larger than the Kondo temperature, the anomalous magnetotransport properties are recovered.

DOI: 10.1103/PhysRevLett.102.046801 PACS numbers: 73.20.Hb, 73.23.−b, 81.05.Uw

Graphene is a two-dimensional material made of carbon atoms arranged in a hexagonal lattice. Its structural stability and unusual electronic properties [1–6] make it an excellent candidate for technological applications. The low-energy electronic structure corresponds to massless, chiral, fermionic quasiparticles described by the Dirac equation. It is also a semimetal that can be globally or locally doped with electrons or holes using gate electrodes. These characteristics triggered intense activity that ranges from the search of new devices to the study of new scenarios for Dirac fermions [5,6]. Important advances have been made in the preparation and characterization of graphene. One of the ongoing goals is to incorporate spintronic effects which requires the development of simple tools for the manipulation and control of the carrier's spins. There are already some advances in this direction, like the injection of a spin-polarized current from ferromagnetic electrodes [7,8]. There are also some theoretical proposals involving the use of edge states to transport spin-polarized currents [9,10]. However, the properties of graphene with magnetic impurities, atoms or molecules, have received less attention. Previous works using mean field approaches already pointed out the unusual behavior of some properties as well as the possibility of controlling the magnetic structure of the impurity with electric fields [11–13]. The magnetic screening of an impurity spin, the Kondo effect, in systems with graphenelike pseudogaps has also been analyzed by several authors [14–16].

In this Letter we address the problem of graphene with magnetic impurities and show that the peculiar electronic properties of this system lead to some interesting new effects. In particular, we show the potential use of these impurities to inject and generate spin-polarized currents. When an impurity is adsorbed on top of a carbon atom, the impurity levels acquire a finite lifetime; that is, the spectral function shows broad peaks. In the undoped case and for realistic parameters, the impurity behaves as a free spin at low temperatures, and we show that with a small magnetic field, such that the Zeeman energy is larger than the thermal energy $k_B T$, a *nonmagnetic* scanning tunneling microscope (STM) tip can be used to inject spin-polarized electrons with an extraordinary efficiency. In this regime we also show that the bulk transport properties present interesting features: in the absence of electron-hole symmetry and with a finite impurity concentration there is a large magnetoresistance and the transport current is spin-polarized. Conversely, a magnetic impurity in doped graphene leads to the Kondo effect. While in general the Kondo temperature $T_K$ is small due to the small density of states at the Fermi energy of graphene, in some cases it could be well above the experimentally accessible limits.

Our starting point is the Anderson model describing an impurity with a single orbital of energy $\varepsilon_d$ and Coulomb repulsion $U$ hybridized with the conduction electron states with a matrix element $V_{\mathrm{hyb}}$. The Hamiltonian of the system is then $H = H_{\mathrm{imp}} + H_{\mathrm{graph}} + H_{\mathrm{hyb}}$, where the first term is given by

$$H_{\mathrm{imp}} = \sum_{\sigma} (\varepsilon_d - \sigma \mu B) d_\sigma^\dagger d_\sigma + U d_\uparrow^\dagger d_\uparrow d_\downarrow^\dagger d_\downarrow. \quad (1)$$

Here $d_\sigma^\dagger$ creates an electron with spin $\sigma$ at the impurity state and $\mu B$ is the Zeeman energy shift due to an external in-plane magnetic field $B$. The Hamiltonian of the graphene layer is

$$H_{\mathrm{graph}} = -t \sum_{\boldsymbol{k},\sigma} [\phi(\boldsymbol{k}) a_{\boldsymbol{k}\sigma}^\dagger b_{\boldsymbol{k}\sigma} + \phi^*(\boldsymbol{k}) b_{\boldsymbol{k}\sigma}^\dagger a_{\boldsymbol{k}\sigma}], \quad (2)$$

where $a_{\boldsymbol{k}\sigma}^\dagger$ and $b_{\boldsymbol{k}\sigma}^\dagger$ create electrons with spin $\sigma$ and wave vector $\boldsymbol{k}$ on sublattices $A$ and $B$, respectively. The hopping matrix element $t$ is of the order of 2.7 eV [6] and $\phi(\boldsymbol{k}) = \sum_j e^{i\boldsymbol{k}\cdot\boldsymbol{\delta}_j}$ with $\{\boldsymbol{\delta}_j\}$ the three vectors connecting one site with its nearest neighbors. As a result there are two bands of width $3t$ that touch each other at the corners of the

 

Brillouin zone (Dirac point). Finally, assuming that the impurity is adsorbed on a site of sublattice $A$, the hybridization Hamiltonian is $H_{\rm hyb} = \frac{V_{\rm hyb}}{\sqrt{N}} \sum_{k\sigma} [a^\dagger_{k\sigma} d_\sigma + d^\dagger_\sigma a_{k\sigma}]$, with $N$ the number of unit cells in the sample.

One of the main ingredients that determines the nature of the solution is the local density of states of the host material. Close to the Dirac point ($E = 0$), the local density of states, per atom and spin, can be approximated by $\rho(E) = \alpha |E|$ with $\alpha = A_{\rm uc}/2\pi\hbar^2 v_F^2$, where $A_{\rm uc}$ is the unit cell area and $v_F$ is the Fermi velocity. In what follows we use this form with a high energy cutoff $D$. The other relevant parameters ($\varepsilon_d$, $U$, $V_{\rm hyb}$) depend on the nature of the impurity; in particular, $U$ is of the order of a few eVs for transition metal impurities and smaller for molecules. We solve the problem using the extensions of Wilson's numerical renormalization group (NRG) method that allow us to describe a nonconstant density of states for the host material and to improve the accuracy of the high energy features [15,17]. We have studied this model numerically for a wide range of parameters. In what follows we will focus on the localized spin regime where the average number of electrons in the impurity level is of the order of 1.

In Fig. 1(a) we present a color map of the impurity spectral density $A(\omega)$ for the undoped case—the Fermi energy $E_F$ lying at the Dirac point. The maximums of $A(\omega)$ are shifted from the bare parameters $\varepsilon_d$ and $\varepsilon_d + U$ shown in the figure with dashed lines. While for a general $\rho(E)$ some shifts are expected, here the shifts are large and the energy difference between the peaks is smaller than $U$. This is due to the interplay between a Hartree correction and the hybridization self-energy [12]. Figures 1(b) and 1(c) show the impurity spectral functions for two different values of $\varepsilon_d$. Note the absence of a Kondo peak at $E_F$. These spectral densities could be measured with a STM where electrons from the microscope tip tunnel to the impurity sensing the local density of states. If the resonant level is close to the Dirac point ($|\varepsilon_d| \lesssim 1$ eV) the STM can measure the resonance. In general there is some leaking of electrons that tunnel to the substrate generating Fano structures. The STM differential conductance at low temperatures is then given by [18]

$$G(V_b) = \frac{4e^2}{\pi\hbar} \tilde{t}^2 \rho_t A_{\rm STM}(E_F + eV_b), \tag{3}$$

where $V_b$ is the voltage drop from the tip to the sample, and $\rho_t$ is the tip density of states at the Fermi energy. The quantity $A_{\rm STM}(E)$ is the spectral function of the operator $(t_c \psi^\dagger_\sigma + t_d d^\dagger_\sigma)/\tilde{t}$, $t_c$ and $t_d$ are matrix elements for the tunneling of an electron from the tip to the conduction band states and to the impurity orbital, respectively, $\tilde{t} = (t_c^2 + t_d^2)^{1/2}$, and $\psi^\dagger_\sigma$ is the field operator that creates an electron in a graphene state centered below the tip. In what follows we consider that the tip is on top of the impurity and for simplicity we take $\psi^\dagger_\sigma = N^{-1/2} \sum_{k\sigma} a^\dagger_{k\sigma}$. Even for $t_c \simeq t_d$ the effect of $t_c$ is very small due to the smallness of $\rho(E \sim E_F)$, see Fig. 1, and the STM gives direct information of the impurity spectral density.

In the presence of an external magnetic field the impurity is polarized and the spectral densities become spin dependent. In Fig. 2 we present results obtained at low temperatures and low fields. Almost all the weight of the spin-resolved spectral densities is transferred to a single

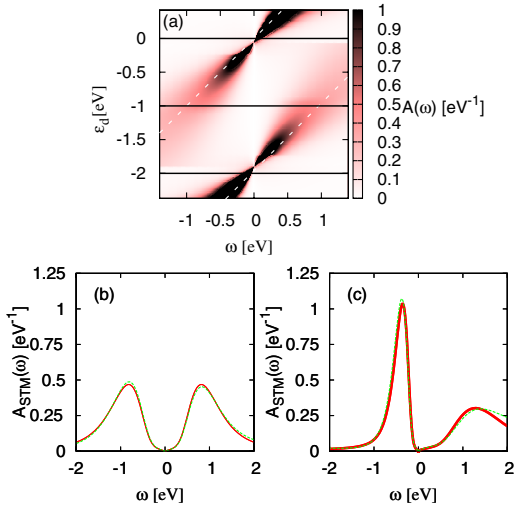


FIG. 1 (color online). (a) Color map of the spectral density of a magnetic impurity on graphene. Parameters are $U = 2$ eV, $V_{\rm hyb} = 1$ eV. (b) STM spectra at the impurity for $t_c/t_d = 0$ (solid lines) and $t_c/t_d = 0.3$ (dashed lines). Here $\varepsilon_d = -1$ eV. (c) Same as (b) with $\varepsilon_d = -0.5$ eV and $t_c/t_d = 0, 1.0$.

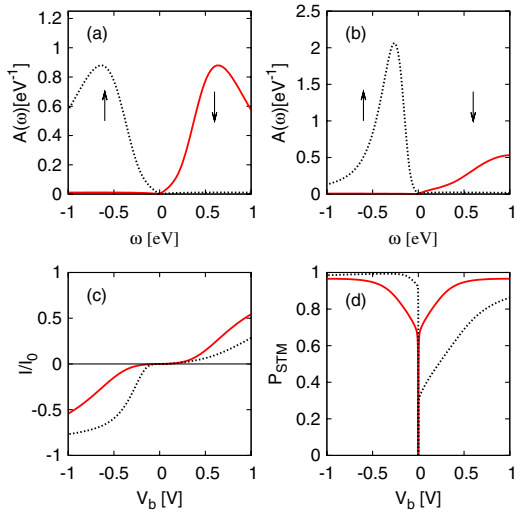


FIG. 2 (color online). (a) Impurity spectral density for the undoped case in the presence of a small magnetic field $\mu B = 70$ $\mu$eV for the spin-up (dashed line) and spin-down (solid line) projections. Here $V_{\rm hyb} = 1.4$ eV, $\varepsilon_d = -U/2$ and the other parameters are as in Fig. 1. (b) Same as (a) for $\varepsilon_d = -0.5$ eV. (c) STM current and (d) current polarization as a function of the bias voltage $V_b$ for the spectral densities shown in (a) (solid line) and (b) (dashed line).

peak at the renormalized energies $\tilde{\varepsilon}_d$ (for the spin-up) and $\tilde{\varepsilon}_d + \tilde{U}$ (for the spin-down). For the small magnetic field used in the calculation the Zeeman shifts of the peaks are not appreciable. These results suggest that the spin dependent STM differential conductance at high voltages becomes very different for the two spin orientations. To estimate the current of spin-$\sigma$ electrons, $I_\sigma$, we integrate the spin dependent differential conductance. The total current $I = I_\uparrow + I_\downarrow$, in units of $I_0 = 4e\tilde{t}^2\rho_t/\pi\hbar$, and the current polarization $P_{\mathrm{STM}} = (I_\uparrow - I_\downarrow)/I$ are shown in Figs. 2(c) and 2(d), respectively. While the tunneling current $I$ is small, the polarization $P_{\mathrm{STM}}$ can exceed 0.98. As we show below, the possibility of injecting spin-polarized currents is not restricted to the undoped case.

In the case of doped graphene $E_F$ is shifted from the Dirac point. In Fig. 3 we present results for the impurity spectral density $A(\omega)$ at low temperatures. There is now a Kondo peak at $E_F$. Following Langreth [19], $A(E_F) = \sin^2(\pi\tilde{n}_d/2)/\pi\Gamma$ where $\tilde{n}_d$ is the total charge displaced by the impurity and $\Gamma = \pi\rho(E_F)V_{\mathrm{hyb}}^2$. Our NRG results reproduce well this exact result. In Fig. 3(c) we present results for the impurity charge $n_d$ versus $\varepsilon_d$. The impurity charge changes when the renormalized energies $\tilde{\varepsilon}_d$ and $\tilde{\varepsilon}_d + \tilde{U}$ cross $E_F$ and the plateau corresponding to a localized spin in the impurity, $n_d \sim 1$, is narrowed as $V_{\mathrm{hyb}}$ increases. This narrowing should not be interpreted as a reduction of the effective repulsion. As we show below, the Kondo temperature is determined by the bare parameter $U$.

We calculate the impurity spin susceptibility $\chi(T)$, that at low temperatures shows universal behavior, and extract $T_K$ using Wilson's criterion $T_K\chi(T_K)/\mu^2 = 0.025$. The results are shown in Fig. 3(d) where $\log(T_K)$ as a function of $\varepsilon_d$ shows the usual quadratic behavior with a minimum at the center of the $n_d \sim 1$ plateau and a curvature determined by the bare interaction $U$. For a given set of impurity parameters, $T_K$ varies with doping, or gate voltage, approaching zero for the undoped case.

The transport properties of graphene are peculiar in many aspects, and it is interesting to study the effect of adsorbed magnetic impurities. In what follows we present results for the resistivity $\rho_{\mathrm{imp}}(T)$ due to these impurities in the low impurity concentration ($c_{\mathrm{imp}}$) regime. Using the general expression for the conductivity in graphene [20,21] and evaluating the band propagators in the Born approximation we obtain, to first order in $c_{\mathrm{imp}}$,

$$\rho_{\mathrm{imp}}(T) = \rho_0 V_{\mathrm{hyb}}^2 \left[ \int \left( -\frac{\partial f(\omega)}{\partial \omega} \right) \frac{|\omega|}{A(\omega)} d\omega \right]^{-1}, \quad (4)$$

where $\rho_0 = \pi c_{\mathrm{imp}} h/e^2$. The general temperature dependence of the resistivity in the different regimes requires the numerical evaluation of the integral. As shown in Fig. 4, for the undoped case the resistivity is temperature independent while for the doped case we obtain the usual Kondo behavior. The NRG results can be qualitatively reproduced performing some simple approximations. In the undoped case the spin dependent low frequency impurity spectral density is given by $A_\sigma(\omega) \simeq \alpha V_{\mathrm{hyb}}^2 |\omega| [(1 - n_{d\bar{\sigma}})/\varepsilon_d^2 + n_{d\bar{\sigma}}/(\varepsilon_d + U)^2]$ where $n_{d\sigma}$ is the number of spin $\sigma$ electrons in the impurity orbital [22]. For the sake of simplicity let us consider first the case $\varepsilon_d = -U/2$ for which $n_{d\sigma} = \frac{1}{2}$; the resistivity is then given by $\rho_{\mathrm{imp}}(T) = \rho_0 \alpha V_{\mathrm{hyb}}^4/\varepsilon_d^2$. This result corresponds to impurities generating a short-range potential of amplitude $\Delta \propto V_{\mathrm{hyb}}^2/|\varepsilon_d|$.

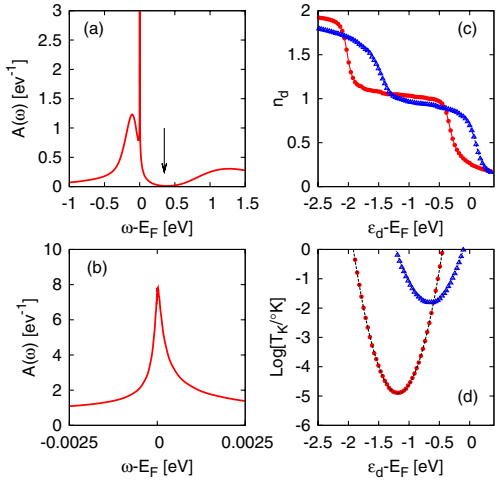


FIG. 3 (color online). (a) Impurity spectral density for the doped case ($E_F = -0.35$ eV). The arrow indicates the position of the Dirac point. (b) Detail of the Kondo peak. (c) Impurity occupation as a function of the level energy: $V_{\mathrm{hyb}} = 1.4$ eV and $E_F = -0.35$ eV (filled circles), $V_{\mathrm{hyb}} = 1.75$ eV and $E_F = 0.35$ eV (filled triangles). The local interaction is in both cases $U = 2$ eV. (d) Kondo temperature versus $\varepsilon_d$ for the parameters of (c). The lines are parabolic fits.

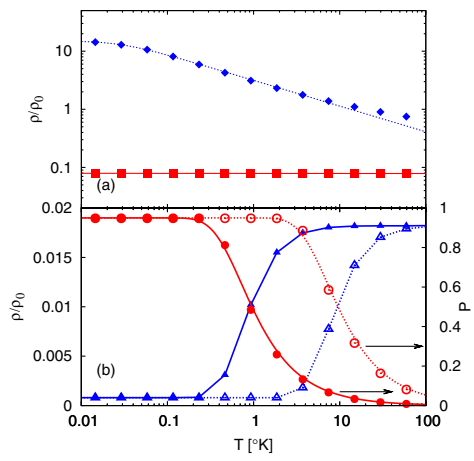


FIG. 4 (color online). (a) Resistivity versus temperature for doped ($E_F = -0.35$ eV, solid diamonds) and undoped graphene (solid squares) for $B = 0$, $U = 2$ eV, $V_{\mathrm{hyb}} = 1.4$ eV, and $\varepsilon_d = -0.63$ eV. Doped graphene shows Kondo scaling of the resistivity indicated by the dotted line. (b) Resistivity (triangles) and current polarization (circles) versus temperature. Undoped graphene, $\mu B = 70$ $\mu$eV (solid symbols) and $\mu B = 700$ $\mu$eV (open symbols). Other parameters are $U = 3.5$ eV and $\varepsilon_d = -0.5$ eV.

In the absence of electron-hole symmetry ($\varepsilon_d \neq -U/2$) the system presents a large magnetoresistance due to the difference in the scattering rate of the two spin channels. The contribution of each spin is given by twice the right-hand side of Eq. (4) with $A(\omega)$ replaced by $A_\sigma(\omega)$, and the total resistivity is

$$\rho_{\mathrm{imp}}(T, B) = \rho_{\mathrm{imp}}(T, B = 0)[1 - \gamma^2 m^2(T, B)], \qquad (5)$$

with $m(T, B) = (n_{d\uparrow} - n_{d\downarrow})$ and for $n_d = 1$, $\gamma = [(\varepsilon_d + U)^2 - \varepsilon_d^2]/[(\varepsilon_d + U)^2 + \varepsilon_d^2]$. The current polarization is $P \equiv (I_\uparrow - I_\downarrow)/I = \gamma m(T, B)$. These expressions are in good qualitative agreement with the numerical results shown in Fig. 4(b). The actual magnetoresistance and the degree of polarization of the current in bulk graphene will depend on the presence and intensity of additional scattering mechanisms. For the magnetoresistance to be observable, the scattering rate due to other mechanisms should be smaller than the one due to the impurities; that is, the impurities should be adsorbed on clean graphene.

For the doped case the Kondo screening in the $T \to 0$ limit gives

$$\rho_{\mathrm{imp}}(0) = \frac{h}{e^2} \frac{c_{\mathrm{imp}} \sin^2(\pi \tilde{n}_d/2)}{\pi n}, \qquad (6)$$

where $n$ is the number of carriers per carbon atom. In the unitary limit, the resistivity is just determined by the ratio $c_{\mathrm{imp}}/n$. In the limit $T \gg T_K$ we recover the resistivity characteristic of potential scattering defects. The temperature dependence of the resistivity, for $T \lesssim T_K$, shows the universal Kondo behavior [23].

In summary, we have numerically solved the problem of a magnetic impurity in graphene and analyzed the effect of external in-plane magnetic fields. We find that as $\varepsilon_d$ varies, the region of stability for a localized spin ($n_d \sim 1$) is narrowed and shifted with respect to the $V_{\mathrm{hyb}} \to 0$ limit, in qualitative agreement with mean field results [12]. Kondo screening of the impurity spin occurs at low temperatures for the doped case. The Kondo temperature $T_K$ decreases exponentially with decreasing doping, and for the undoped case the impurity behaves as a free spin down to zero temperature. We find very little Fano distortions in the STM spectrum that consequently gives a direct measurement of the impurity spectral densities. Our central results concern the effect of magnetic fields: for zero or low doping, low $T_K$, the condition $T, T_K < \mu B$ is accessible at moderate values of the external field $B$. In this regime the impurity spin is polarized and a nonmagnetic STM tip can be gated to inject a spin-polarized current; that is, the impurity acts as a spin valve. The magnetic field controls the degree and the axis of the spin polarization. In this regime, a finite impurity concentration leads to large magnetotransport effects in bulk graphene: for small values of $|\varepsilon_d - E_F|$ the system shows large magnetoresistance and spin-polarized currents. All these effects are unique to graphene: they require $V_{\mathrm{hyb}}^2/|\varepsilon_d|$ to be large and the spin to be free at low temperatures, conditions that are never reached simultaneously in ordinary metals. Our main results are robust even in the presence of defects or other impurities that may change the structure of the pseudogap and the nature of the magnetic screening. However, for magnetic impurities close to one of these defects, new features are expected to appear in the STM spectra that will depend on the nature of the defect.

We acknowledge financial support from ANPCyT Grants No. 13829/03, No. 483/06, and No. 482/06 and CONICET PIP 5254/05.

[1] K. S. Novoselov, A. K. Geim, S. V. Morozov, D. Jiang, Y. Zhang, S. V. Dubonos, I. V. Grigorieva, and A. A. Firsov, Science **306**, 666 (2004).
[2] K. S. Novoselov, A. K. Geim, S. V. Morozov, D. Jiang, M. I. Katsnelson, I. V. Grigorieva, S. V. Dubonos, and A. A. Firsov, Nature (London) **438**, 197 (2005).
[3] M. I. Katsnelson, K. S. Novoselov, and A. K. Geim, Nature Phys. **2**, 620 (2006).
[4] K. S. Novoselov, Z. Jiang, Y. Zhang, S. V. Morozov, H. L. Stormer, U. Zeitler, J. C. Maan, G. S. Boebinger, P. Kim, and A. K. Geim, Science **315**, 1379 (2007).
[5] A. K. Geim and K. S. Novoselov, Nature Mater. **6**, 183 (2007).
[6] A. H. Castro Neto, F. Guinea, N. M. R. Peres, K. S. Novoselov, and A. K. Geim, arXiv:0709.1163.
[7] H. Haugen, D. Huertas-Hernando, and A. Brataas, Phys. Rev. B **77**, 115406 (2008).
[8] N. Tombros, C. Jozsa, M. Popinciuc, H. T. Jonkman, and B. J. van Wees, Nature (London) **448**, 571 (2007).
[9] M. Wimmer, İnanç Adagideli, S. Berber, D. Tománek, and K. Richter, Phys. Rev. Lett. **100**, 177207 (2008).
[10] Y.-W. Son, M. L. Cohen, and S. G. Louie, Nature (London) **444**, 347 (2006).
[11] B. Dora and P. Thalmeier, Phys. Rev. B **76**, 115435 (2007).
[12] B. Uchoa, V. N. Kotov, N. M. R. Peres, and A. H. Castro Neto, Phys. Rev. Lett. **101**, 026805 (2008).
[13] K. Sengupta and G. Baskaran, Phys. Rev. B **77**, 045417 (2008).
[14] D. Withoff and E. Fradkin, Phys. Rev. Lett. **64**, 1835 (1990).
[15] C. Gonzalez-Buxton and K. Ingersent, Phys. Rev. B **57**, 14254 (1998).
[16] M. Vojta, Philos. Mag. **86**, 1807 (2006).
[17] R. Bulla, T. A. Costi, and T. Pruschke, Rev. Mod. Phys. **80**, 395 (2008).
[18] P. S. Cornaglia and C. A. Balseiro, Phys. Rev. B **67**, 205420 (2003).
[19] D. C. Langreth, Phys. Rev. **150**, 516 (1966).
[20] N. M. R. Peres, F. Guinea, and A. H. Castro Neto, Phys. Rev. B **73**, 125411 (2006).
[21] N. H. Shon and T. Ando, J. Phys. Soc. Jpn. **67**, 2421 (1998).
[22] A. C. Hewson and M. Zuckermann, Phys. Lett. **20**, 219 (1966).
[23] D. Goldhaber-Gordon, J. Göres, M. A. Kastner, H. Shtrikman, D. Mahalu, and U. Meirav, Phys. Rev. Lett. **81**, 5225 (1998).